AGU100 ADVANCING EARTH AND SPACE SCIENCE

Radio Science

RESEARCH ARTICLE
10.1002/2017RS006429

Key Points:
- A novel and efficient integral equation formulation for the analysis of inductive steps including arbitrarily shaped conductor and dielectrics is presented
- Efficient Green's functions evaluation is shown

Correspondence to:
F. D. Quesada Pereira,
fernando.quesada@upct.es

Citation:
QuesadaPereira, F. D., Gómez Molina, C., Alvarez Melcon, A., Boria, V. E., & Guglielmi, M. (2018). Novel spatial domain integral equation formulation for the analysis of rectangular waveguide steps close to arbitrarily shaped dielectric and/or conducting posts. *Radio Science*, *53*, 406–419. https://doi.org/10.1002/2017RS006429

Received 7 AUG 2017
Accepted 25 FEB 2018
Accepted article online 1 MAR 2018
Published online 6 APR 2018

Novel Spatial Domain Integral Equation Formulation for the Analysis of Rectangular Waveguide Steps Close to Arbitrarily Shaped Dielectric and/or Conducting Posts

F. D. Quesada Pereira[1], C. Gómez Molina[1], A. Alvarez Melcon[1], V. E. Boria[2], and M. Guglielmi[2]

[1]Departamento de Tecnologías de la Información y las Comunicaciones, Universidad Politécnica de Cartagena, Cartagena, Spain, [2]Instituto de Telecomunicaciones y Aplicaciones Multimedia, Universidad Politécnica de Valencia, Valencia, Spain

Abstract In this paper, a novel integral equation formulation expressed in the spatial domain is proposed for the analysis of rectangular waveguide step discontinuities. The important novelty of the proposed formulation is that which allows to easily take into account the electrical influence of a given number of arbitrarily shaped conducting and dielectric posts placed close to the waveguide discontinuity. For the sake of simplicity, and without loss of generality, the presented integral equation has been particularized and solved for inductive rectangular waveguide geometry. In this case, the integral equation mixed-potentials kernel is written in terms of parallel plate Green's functions with an additional ground plane located on the waveguide step. Therefore, the unknowns of the problem are reduced to an equivalent magnetic surface current on the step aperture and equivalent magnetic and electric surface currents on the dielectric and conducting posts close to the discontinuity. The numerical solution of the final integral equation is efficiently computed after the application of acceleration techniques for the slowly convergent series representing the Green's functions of the problem. The numerical method has been validated through several simulation examples of practical microwave devices, including compact size band-pass cavity filters and coupled dielectric resonators filters. The results have been compared to those provided by commercial full-wave electromagnetic simulation software packages, showing in all cases a very good agreement, and with substantially enhanced numerical efficiencies.

1. Introduction

An efficient analysis and electrical characterization of waveguide discontinuities (Marcuvitz, 1964) is a paramount requirement for the electromagnetic characterization of passive components, and for the design of a wide class of microwave devices such as filters, multiplexers, power dividers, and combiners (Mrvic et al., 2016). Most of these devices are built as a concatenation of different waveguides and cavity sections, which are connected through waveguide discontinuities. This is the main motivation that drives the microwave engineering community to develop new techniques specially tailored for the analysis of waveguide discontinuities. Some of these numerical methods are quite general such as Finite Elements (Salazar Palma et al., 1998) or Finite Differences in Time Domain (FDTD) (Peterson et al., 1998a). Besides the characterization of waveguide discontinuities, these general techniques cover the analysis of a wide range of different types of practical microwave structures, at the expense of losing computational efficiency. On the other hand, full-wave techniques such as those based on modal methods or integral equations (Arcioni et al., 1997; Guglielmi & Newport, 1990) are very fast and require lower computational costs. Among these techniques, those based on mode-matching formulations have shown to be very efficient in the characterization of waveguide steps (Catina et al., 2005; Mohsen & Kian, 2017). Nevertheless, the previous methods are limited to the analysis of canonical geometries or has serious difficulties when dealing with arbitrarily shaped conducting and/or dielectric bodies close to the waveguide discontinuity under study.

An alternative technique to these previous techniques is the integral equation formulated in the spatial domain (Perez Soler et al., 2007; Quesada Pereira et al., 2006, 2011). The advantage of this technique is that it can treat more general structures composed of complex-shaped metallic posts or homogeneous material

bodies, once the relevant Green's functions of the problem are efficiently computed in the spatial domain. However, in these previous contributions waveguide steps and coupling windows are treated as general metallic objects. This imposed an important limitation to the waveguide components that could be treated with such formulations. In fact, the whole structure was limited to be confined into a single waveguide region, containing inside the rest of metallic posts or homogeneous material bodies.

With the previous considerations in mind, a novel integral equation formulation for the analysis of waveguide discontinuities is presented in this paper. The main contribution with respect to these previous works is that the waveguide discontinuity is not treated as a general metallic object. Instead, the discontinuity is treated as an aperture problem. The main advantage of this approach is that it introduces increased flexibility in the structures that can be treated. In fact, the formulation of the discontinuity as an aperture problem allows the separation of the whole structure in two different simpler problems. Consequently, two different waveguide regions, which can be arbitrarily configured, can be effectively connected to compose a very general microwave device. Note that this ability to connect two different and very complex structures was not possible with the two previously cited works.

The proposed numerical method represents a compromise between the aforementioned general and specialized analysis techniques. The proposed formulation is quite general, in the sense that it allows the electromagnetic characterization of a wide range of complex waveguide discontinuities, that involve an arbitrary number of complex-shaped conducting and/or homogenous objects in their vicinity. However, the use of specialized waveguide Green's functions in the kernel of the integral equation is able to effectively reduce the unknowns of the problem and keep high efficiency in the full-wave analysis of the structures under study. The proposed integral equation formulation could be adapted to different kinds of waveguide discontinuities. Nevertheless, for the sake of simplicity, in this work the formulation has been particularized to the study of only rectangular waveguide inductive step discontinuities that are considered to be invariant over one dimension, leaving for a future research the analysis of the capacitive and two-dimensional cases. In this situation, the original integral equation formulation written in terms of surface integrals is reduced to a contour integral equation formulation. Many works can be found in the technical literature dealing with contour integral equations, such as Stumpf and Leone (2009), Wei et al. (2008), and Zhao et al. (2014), where power-ground planes connected to electronic packages are efficiently analyzed. However, the kind of studied problems and the integral equation implementation in this work are different. The integral equation formulation could also be applied to the analysis of waveguide steps including arbitrarily shaped inhomogeneous dielectric obstacles modeled by means of a Volume Integral Equation formulations (Hu et al., 2016).

This work is organized as follows. First, the general type of problem (an inductive step discontinuity with arbitrarily shaped conducting and homogenous material posts on each side) to be solved in this paper, is described. Then, the procedure employed for obtaining a system of integral equations that characterizes the structure under analysis is outlined. This procedure is based on dividing the original structure into different equivalent problems after the application of the Surface Equivalent Principle, and then enforcing appropriate boundary conditions. Details on the Green's functions, used in the kernel of the formulated integral equations, are provided in a specific subsection. After that, some comments on how the resulting integral equation is efficiently solved by the Method of Moments (MoM) are included. Next, special attention will be paid to the particular expressions for computing the scattering parameters of a given structure using this integral novel equation formulation. After the theoretical aspects have been carefully discussed, some validation examples are presented in order to check the utility and computational efficiency of the proposed integral equation. Finally, some conclusions are provided and future research work on this topic is also proposed.

2. Integral Equation Formulation

In this section, the novel integral equation formulation used for the analysis of rectangular waveguide discontinuities is summarized. For the sake of simplicity, the integral equation is particularized for the study of inductive step discontinuities, considering the geometry of the problem to be invariant along the y axis, whose widths are a_1 and a_2, as shown in Figure 1. Due to the inductive nature of the considered structure, the excitation, the electromagnetic fields, and unknowns do not change along one dimension, in our particular case the y axis, reducing a 3-D problem to a 2-D one. Despite this simplification, the implemented technique can be used for the design of practical inductive waveguide components, commonly used in satellite applications (Cameron et al., 2007). Although the integral equation formulation could be applied to more general step

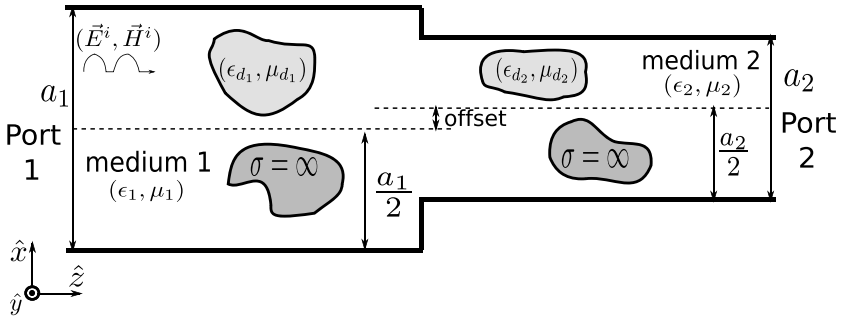

Figure 1. Original problem, invariant along the *y* axis, showing an inductive step discontinuity between two rectangular waveguides with different widths (a_1, a_2). An arbitrarily shaped conducting and dielectric post $((\epsilon_{d_1}, \mu_{d_1})$ in waveguide 1, and $(\epsilon_{d_2}, \mu_{d_2})$ in waveguide 2) are placed inside each rectangular waveguide.

geometry, this fact allows a simpler and faster numerical solution of the problem. An unlimited number of arbitrarily shaped conducting and/or homogeneous material bodies could be considered inside each waveguide. Nevertheless, without loss of generality, the equations will be written for a sample configuration with only a homogeneous object and a conducting post placed on each side of the discontinuity, as represented in Figure 1.

In this waveguide structure it is assumed that the excitation will be the fundamental mode (TE_{10}) of the input rectangular waveguide 1, filled with a homogeneous and isotropic medium 1 (ϵ_1, μ_1), and traveling along the *z* axis toward the discontinuity. As shown in Figure 1, this mode impinges on a homogenous body with constitutive parameters $(\epsilon_{d_1}, \mu_{d_1})$, a perfect electric-conducting body $(\sigma = \infty)$ and the waveguide step discontinuity. Through the aperture formed by this inductive discontinuity, the electromagnetic fields are coupled to the output waveguide, where another homogeneous material body $(\epsilon_{d_2}, \mu_{d_2})$ and a perfect electric conductor post are placed inside. In this last case, the output waveguide is filled with homogeneous constitutive parameters (ϵ_2, μ_2).

In order to study the electrical response of the structure shown in Figure 1, we propose to employ an efficient integral equation formulation. The first step for writing this integral equation will be to split the aforementioned original problem into two coupled equivalent ones. The first equivalent problem corresponds to the input waveguide 1, as can be seen in Figure 2.

For this problem, the conducting post is replaced by an induced surface electric current density, namely, $\vec{J}_{c_1}$, whereas surface equivalent electric and magnetic current densities, $\vec{J}_{d_1}$ and $\vec{M}_{d_1}$, substitute the homogeneous material body placed inside this input waveguide. In both cases, the inner region of the arbitrarily shaped bodies is filled with the constitutive parameters corresponding to medium 1 (ϵ_1, μ_1), while the electromagnetic fields are assumed to be null inside those regions $(\vec{E} = 0, \vec{H} = 0)$. Moreover, an infinite ground plane located at the discontinuity between waveguides, namely, at $z = 0$ from now on, is used in order to separate the two equivalent problems. At this ground plane, in the aperture formed by the step discontinuity, an equivalent surface magnetic current density $\vec{M}_{ap}$ is employed to couple the integral equations formulated for each waveguide region. It is very important to note that the excitation of the original problem, which is the fundamental $TE_{10}^{(1)}$ mode in waveguide1, is no longer valid for the equivalent problem corresponding to the input waveguide. This is because the nullity of the tangential component of the electric field to the ground plane at the interface $z = 0$ will not be automatically fulfilled.

Therefore, the excitation is modified by the addition of its electrical image $\vec{E}^i_{imag}$ with respect to the infinite ground plane at $z = 0$. This image will be a TE_{10} mode traveling backward to the input port, but with an opposite sign. This last wave, together with the original excitation, could be considered as a standing wave $(\vec{E}^i_{eq}, \vec{H}^i_{eq})$ inside the input waveguide problem. Finally, the electrical influence of the rectangular waveguide side walls will be taken into account in the kernel of the proposed integral equation formulation, by means of the well-known parallel plate Green's functions with width a_1.

A second equivalent problem is now formulated for the region corresponding to the output waveguide (see Figure 3), following a similar procedure to that one of the input waveguides. In this case, the homogenous body $(\epsilon_{d_2}, \mu_{d_2})$ is replaced by surface equivalent electric $\vec{J}_{d_2}$ and magnetic $\vec{M}_{d_2}$ currents, whereas the conductor

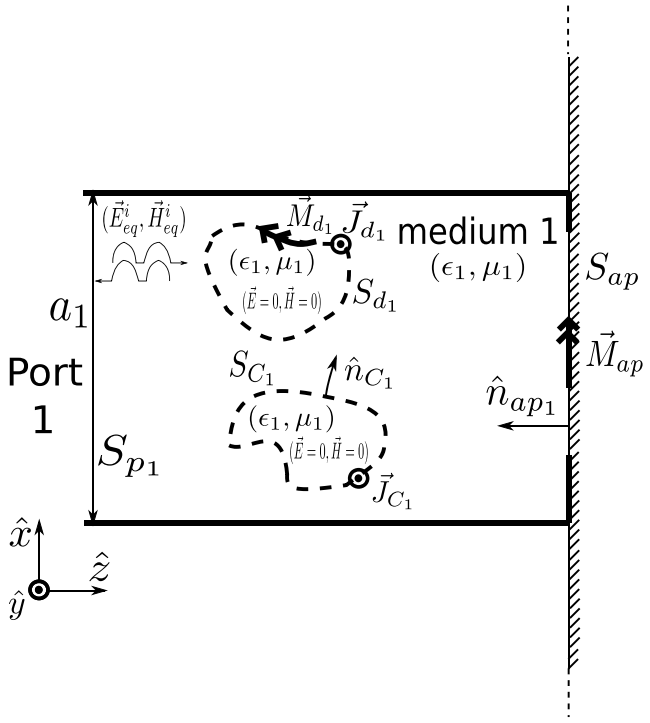

Figure 2. Equivalent problem 1 corresponding to the input rectangular waveguide 1.

is modeled by the induced surface electric current $\vec{J}_{C_2}$ on its contour. As before, the inner region of the homogeneous and conducting bodies is filled with the medium of waveguide 2 (ϵ_2, μ_2), since the electromagnetic fields are null inside ($\vec{E} = 0, \vec{H} = 0$). The integral equation excitation does not explicitly appear in this second equivalent problem, since the excitation mode is launched in waveguide1. Both equivalent problems are coupled to each other by means of the surface equivalent magnetic current $\vec{M}_{ap}$ defined on the discontinuity aperture. Finally, the imposition of the boundary conditions at the walls of the output waveguide is achieved by using in the kernel of the integral equation the parallel plate Green's functions with width a_2 (see Figure 3).

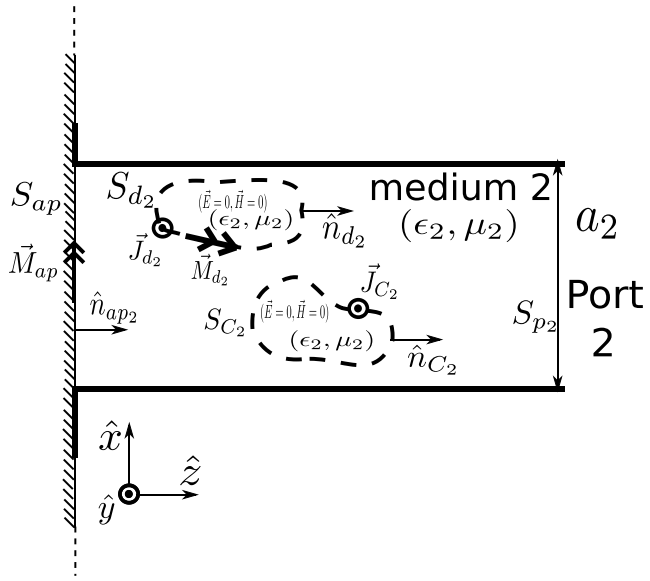

Figure 3. Equivalent problem 2 corresponding to the output rectangular waveguide 2.

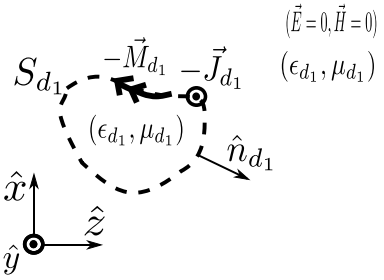

Figure 4. Inner equivalent problem 3 corresponding to the arbitrarily shaped dielectric post inside waveguide 1.

The electromagnetic characterization of the homogenous material objects inside the input and output waveguides, after the application of the Surface Equivalence Principle (Balanis, 1989), requires an additional internal equivalent problem for both of them. In Figure 4 this internal equivalent problem is depicted, corresponding to the material body inside the input waveguide. In this problem, the whole space surrounding the homogenous body is replaced by an unbounded medium of constitutive parameters equal to those filling the inner part of the object $(\epsilon_{d_1},\mu_{d_1})$. In the external region, the electromagnetic fields are assumed to be null for this equivalent problem $(\vec{E}=0,\vec{H}=0)$. Finally, enforcing the continuity of the electric and magnetic fields, tangent to the homogeneous body contour, this internal equivalent problem is coupled to the previously described ones. A similar procedure will be followed for the internal equivalent problem of the homogenous post inside the output waveguide.

Once the different equivalent problems used for the electromagnetic analysis of the given sample structure have been described, the next step is to write the whole system of coupled integral equations that will allow to compute the electrical response, after that their solution will be found by the application of the well-known MoM. Three integral equations are written for the equivalent problem corresponding to each input and output rectangular waveguide. One of them is an Electric Field Integral Equation that enforces the nullity of the total tangential electric field on the surface S_{C_1} and S_{C_2} of the arbitrarily shaped conducting posts. The homogenous material bodies after the application of the Surface Equivalence Principle require two additional coupled integral equations, enforcing the continuity of the tangential electric and magnetic fields components across their contours S_{d_1} and S_{d_2} (also called PMCHWT choice, Poggio & Miller, 1973). Finally, the two waveguide equivalent problems are coupled by means of an additional integral equation that imposes the continuity of the magnetic field components, which are tangent to the aperture surface S_{ap} on the step discontinuity. Taking into account these considerations, the full system of integral equations for the analysis of the structure depicted in Figure 1 can be written as

$$\begin{aligned}
&\hat{n}_{C_1}\times\left(\vec{E}^{i}_{\text{eq}}+\vec{E}^{s}_{\text{PPW}_1}(\vec{J}_{C_1},\vec{J}_{d_1},\vec{M}_{d_1},\vec{M}_{\text{ap}})\right)=0, \qquad \text{On } S_{C_1}\\
&\hat{n}_{d_1}\times\left(\vec{E}^{i}_{\text{eq}}+\vec{E}^{s}_{\text{PPW}_1}(\vec{J}_{C_1},\vec{J}_{d_1},\vec{M}_{d_1},\vec{M}_{\text{ap}})\right)=\hat{n}_{d_1}\times\vec{E}^{s}_{\text{int}_1}(-\vec{J}_{d_1},-\vec{M}_{d_1}), \qquad \text{On } S_{d_1}\\
&\hat{n}_{d_1}\times\left(\vec{H}^{i}_{\text{eq}}+\vec{H}^{s}_{\text{PPW}_1}(\vec{J}_{C_1},\vec{J}_{d_1},\vec{M}_{d_1},\vec{M}_{\text{ap}})\right)=\hat{n}_{d_1}\times\vec{H}^{s}_{\text{int}_1}(-\vec{J}_{d_1},-\vec{M}_{d_1}), \qquad \text{On } S_{d_1}
\end{aligned} \tag{1}$$

for the equivalent problem inside the input waveguide,

$$\hat{n}_{\text{ap}_1}\times\left(\vec{H}^{i}_{\text{eq}}+\vec{H}^{s}_{\text{PPW}_1}(\vec{J}_{C_1},\vec{J}_{d_1},\vec{M}_{d_1},\vec{M}_{\text{ap}})\right)=\hat{n}_{\text{ap}_2}\times\vec{H}^{s}_{\text{PPW}_2}(\vec{J}_{C_2},\vec{J}_{d_2},\vec{M}_{d_2},\vec{M}_{\text{ap}}), \qquad \text{On } S_{\text{ap}} \tag{2}$$

for connecting the two waveguide problems through the aperture, and

$$\begin{aligned}
&\hat{n}_{C_2}\times\vec{E}^{s}_{\text{PPW}_2}(\vec{J}_{C_2},\vec{J}_{d_2},\vec{M}_{d_2},\vec{M}_{\text{ap}})=0, \qquad \text{On } S_{C_2}\\
&\hat{n}_{d_2}\times\vec{E}^{s}_{\text{PPW}_2}(\vec{J}_{C_2},\vec{J}_{d_2},\vec{M}_{d_2},\vec{M}_{\text{ap}})=\hat{n}_{d_2}\times\vec{E}^{s}_{\text{int}_2}(-\vec{J}_{d_2},-\vec{M}_{d_2}), \qquad \text{On } S_{d_2}\\
&\hat{n}_{d_2}\times\vec{H}^{s}_{\text{PPW}_2}(\vec{J}_{C_2},\vec{J}_{d_2},\vec{M}_{d_2},\vec{M}_{\text{ap}})=\hat{n}_{d_2}\times\vec{H}^{s}_{\text{int}_2}(-\vec{J}_{d_2},-\vec{M}_{d_2}), \qquad \text{On } S_{d_2}
\end{aligned} \tag{3}$$

for the equivalent problem inside the output waveguide.

In equations (1)–(3), the terms $\vec{E}^{s}_{\text{PPW}_1}$, $\vec{H}^{s}_{\text{PPW}_1}$, $\vec{E}^{s}_{\text{PPW}_2}$, and $\vec{H}^{s}_{\text{PPW}_2}$ represent the scattered electric and magnetic fields inside the input and output waveguides 1 and 2. The subindex PPW indicates that the scattered fields will be evaluated by means of auxiliary potentials, expressed in terms of the parallel plate Green's functions corresponding to each rectangular waveguide. On the other hand, $\vec{E}^{s}_{\text{int}_1}$, $\vec{H}^{s}_{\text{int}_1}$, $\vec{E}^{s}_{\text{int}_2}$ and $\vec{H}^{s}_{\text{int}_2}$ are the scattered electric and magnetic fields inside the homogenous material objects, placed respectively in the input and output waveguides. These scattered fields are computed after the application of the Surface Equivalence Principle by means of auxiliary potentials, whose kernel is the free space Green's functions of unbounded media with constitutive parameters $(\epsilon_{d_1},\mu_{d_1})$ and $(\epsilon_{d_2},\mu_{d_2})$, respectively. The remaining fields $\vec{E}^{i}_{\text{eq}}$ and $\vec{H}^{i}_{\text{eq}}$ are, respectively, the electric and magnetic standing waves that model the integral equation excitation produced by the input rectangular waveguide fundamental mode $\text{TE}^{(1)}_{10}$.

The electric and magnetic fields in the integral equation formulation are written in the spatial domain using a mixed-potentials form, following these mathematical expressions,

$$\begin{aligned}
\vec{E}^s_{\mathrm{PPW}_q}(x_q,z) &= -j\omega\vec{A}_{\mathrm{PPW}_q}\left(\vec{J}_{C_q}(x'_q,z')\right) - j\omega\vec{A}_{\mathrm{PPW}_q}\left(\vec{J}_{d_q}(x'_q,z')\right) \\
&\quad - \frac{1}{\epsilon_q}\nabla\times\vec{F}_{\mathrm{PPW}_q}\left(\vec{M}_{d_q}(x'_q,z')\right) - \frac{1}{\epsilon_q}\nabla\times\vec{F}_{\mathrm{PPW}_q}\left(\vec{M}_{\mathrm{ap}}(x'_q,z')\right) \\
\vec{H}^s_{\mathrm{PPW}_q}(x_q,z) &= \frac{1}{\mu_q}\nabla\times\vec{A}_{\mathrm{PPW}_q}\left(\vec{J}_{C_q}(x'_q,z')\right) + \frac{1}{\mu_q}\nabla\times\vec{A}_{\mathrm{PPW}_q}\left(\vec{J}_{d_q}(x'_q,z')\right) \\
&\quad - j\omega\vec{F}_{\mathrm{PPW}_q}\left(\vec{M}_{d_q}(x'_q,z')\right) - \nabla\Phi_{m_{\mathrm{PPW}_q}}\left(\vec{M}_{d_q}(x'_q,z')\right) \\
&\quad - j\omega\vec{F}_{\mathrm{PPW}_q}\left(\vec{M}_{\mathrm{ap}}(x'_q,z')\right) - \nabla\Phi_{m_{\mathrm{PPW}_q}}\left(\vec{M}_{\mathrm{ap}}(x'_q,z')\right) \\
\vec{E}^s_{\mathrm{int}_q}(x_q,z) &= -j\omega\vec{A}_{\mathrm{int}_q}\left(-\vec{J}_{d_q}(x'_q,z')\right) - \frac{1}{\epsilon_{d_q}}\nabla\times\vec{F}_{\mathrm{int}_q}\left(-\vec{M}_{d_q}(x'_q,z')\right) \\
\vec{H}^s_{\mathrm{int}_q}(x_q,z) &= \frac{1}{\mu_{d_q}}\nabla\times\vec{A}_{\mathrm{int}_q}\left(-\vec{J}_{d_q}(x'_q,z')\right) \\
&\quad - j\omega\vec{F}_{\mathrm{int}_q}\left(-\vec{M}_{d_q}(x'_q,z')\right) - \nabla\Phi_{m_{\mathrm{int}_q}}\left(-\vec{M}_{d_q}(x'_q,z')\right)
\end{aligned} \tag{4}$$

The different potential functions can be written in terms of the Green's functions corresponding to the equivalent problems, as indicated next

$$\vec{A}_{\mathrm{PPW}_q}\left(\vec{J}(x'_q,z')\right) = \int_S \overline{\overline{G}}_{A_{PPW_q}}(x_q,x'_q,z,z')\cdot\vec{J}(x'_q,z')\,\mathrm{d}C' \tag{5}$$

Equation (5) is the magnetic vector potential evaluated at observation coordinates (x_q,z) (on S_{ap}, S_{C_q}, or S_{d_q}). The source is an equivalent electric surface current $\vec{J}(x'_q,z')$ distributed on S_{C_q} or S_{d_q}, corresponding to the conducting or homogenous objects (primed spatial variables are used to denote the position of the source). It is important to note that the integral equation formulation has been written for a general problem that involves surface integrals. However, in our particular case, due to the inductive symmetry of the proposed examples, which are invariant along the y axis, the surface integrals are reduced to contour integrals. The kernel of the associated integral equation is formed with the magnetic vector potential dyadic Green's function $\overline{\overline{G}}_{A_{PPW_q}}(x_q,x'_q,z,z')$ of a parallel plate waveguide terminated on a ground plane at $z=0$. In all terms, the subindex q represents which rectangular waveguide is considered ($q=1$ for input waveguide, and $q=2$ for output waveguide).

Following a similar notation, we can write the electric vector potential produced by magnetic currents as follows,

$$\vec{F}_{\mathrm{PPW}_q}\left(\vec{M}(x'_q,z')\right) = \int_S \overline{\overline{G}}_{F_{\mathrm{PPW}_q}}(x_q,x'_q,z,z')\cdot\vec{M}(x'_q,z')\,\mathrm{d}C' \tag{6}$$

The kernel of the corresponding integral equation is the electric vector potential dyadic Green's function $\overline{\overline{G}}_{F_{\mathrm{PPW}_q}}(x_q,x'_q,z,z')$ of a parallel plate waveguide that ended in a short circuit at $z=0$. In this expression, the source $\vec{M}(x'_q,z')$ is the equivalent magnetic current source density on the step aperture or on the homogeneous material posts contour.

Finally, the magnetic scalar potential produced by magnetic charges can also be computed using the magnetic scalar potential Green's function $G_{W_{\mathrm{PPW}_q}}(x_q,x'_q,z,z')$, as

$$\Phi_{m_{\mathrm{PPW}_q}}\left(\vec{M}(x'_q,z')\right) = \int_S G_{W_{\mathrm{PPW}_q}}(x_q,x'_q,z,z')\,\frac{\nabla\cdot\vec{M}(x'_q,z')}{-j\omega}\,\mathrm{d}C' \quad . \tag{7}$$

In this case the Green's function is also computed inside a parallel plate region terminated in the ground plane placed at $z=0$. The continuity equation has been used in equation (7) in order to write the magnetic charge density as a function of the surface magnetic current density $\vec{M}(x'_q,z')$.

Table 1
Parallel Plate Green's Functions Components Needed in the Analysis of the Inductive Step Problem Studied in This Paper

–	ξ_q	g_n	f_n
$G^{yy}_{A_{\mathrm{PPW}_o}}$	μ_q	$\sin(k_{x_q}x_q)$	$\sin(k_{x_q}x'_q)$
$G^{xx}_{F_{\mathrm{PPW}_o}}$	ε_q	$\sin(k_{x_q}x_q)$	$\sin(k_{x_q}x'_q)$
$G^{zz}_{F_{\mathrm{PPW}_o}}$	ε_q	$\cos(k_{x_q}x_q)$	$\cos(k_{x_q}x'_q)$
$G_{W_{\mathrm{PPW}_o}}$	$1/\mu_q$	$\cos(k_{x_q}x_q)$	$\cos(k_{x_q}x'_q)$

Note. Since electric and/or magnetic sources are employed to represent material bodies, the conducting posts, and the discontinuity aperture, we need both types of Green's functions.

For the inner equivalent problem of the homogenous material objects, the potential functions $\vec{A}_{\mathrm{int}_q}(\vec{J}(x'_q,z'))$, $\vec{F}_{\mathrm{int}_q}(\vec{M}(x'_q,z'))$, and $\Phi_{m_{\mathrm{int}_q}}(\vec{M}(x'_q,z'))$ are written as $\vec{A}_{\mathrm{PPW}_q}(\vec{J}(x'_q,z'))$, $\vec{F}_{\mathrm{PPW}_q}(\vec{M}(x'_q,z'))$, and $\Phi_{m_{\mathrm{PPW}_q}}(\vec{M}(x'_q,z'))$ in equations (5)–(7). Nevertheless, in this situation, this equivalent problem corresponds to an unbounded homogenous medium with constitutive parameters ϵ_{d_q} and μ_{d_q} (permittivity and permeability of the homogeneous material body inside the rectangular waveguide q). Therefore, the kernel of the associated integral equation is written in terms of simple two-dimensional free space Green's functions in the corresponding medium (Peterson et al., 1998b). This means replacing $\overline{\overline{G}}_{A_{\mathrm{PPW}_q}}(x_q,x'_q,z,z')$, $\overline{\overline{G}}_{F_{\mathrm{PPW}_q}}(x_q,x'_q,z,z')$, and $G_{W_{\mathrm{PPW}_q}}(x_q,x'_q,z,z')$, by $G_{A_{\mathrm{int}_q}}(\vec{\rho}_q,\vec{\rho}'_q)$, $G_{F_{\mathrm{int}_q}}(\vec{\rho}_q,\vec{\rho}'_q)$, and $G_{W_{\mathrm{int}_q}}(\vec{\rho}_q,\vec{\rho}'_q)$, respectively. The expressions of these Green's functions are detailed in the next section.

2.1. Green's Functions of the Equivalent Problems

In this section, the Green's functions needed for the evaluation of the different potentials of the derived integral equation formulation, are collected. First, the components of the dyadic parallel plate Green's function potentials, required for the solution of the system of integral equations, under the assumption that the geometry of the problem has inductive geometry, are described. Moreover, the magnetic scalar potential Green's function for the external equivalent problem in the input and output waveguides is also introduced. Second, the described parallel plate Green's functions are combined with a space image in order to take into account the infinite ground plane that split the original problem into the two different waveguide regions. At the end of the section, the two-dimensional free space Green's functions used for the equivalent problem inside the homogeneous material posts are also given, for the sake of completeness.

Although the integral equation is written in the spatial domain, the parallel plate Green's functions can be formulated either in the spectral or in the spatial domains (Capolino et al., 2005). In the spectral domain, the following series of modal functions are obtained for the parallel plate Green's functions with width a_q

$$G_{\mathrm{PPW}_o}(x_q,x'_q,z,z') = \frac{\xi_q}{2a_q}\sum_{n=0}^{\infty} e_n\, f_n(k_{x_q}x'_q)\, g_n(k_{x_q}x_q)\, \frac{e^{-jk_{z_q}(z-z')}}{jk_{z_q}}$$
$$k_{z_q} = \sqrt{k_q^2 - k_{x_q}^2}, \qquad k_{x_q} = \frac{n\pi}{a_q} \tag{8}$$

where the term $e_n = \begin{cases} 1 & n=0 \\ 2 & n\neq 0 \end{cases}$, f_n and g_n are trigonometric functions, and ξ_q is a constant that depends on the constitutive parameters of the waveguide medium. Also, k_{z_q} is the longitudinal wave number that depends on the medium that fills the corresponding waveguide through $k_q = \omega\sqrt{\epsilon_q\mu_q}$. In Table 1 we list all Green's functions components needed in the analysis of dielectric and/or magnetic posts.

After taking into account the influence of the perfect electric conductor ground plane at $z = 0$ by image theory, the final expressions for the external equivalent problems Green's function components in waveguide regions 1 and 2 can be written as follows:

$$\begin{aligned}
G^{yy}_{A_{\mathrm{PPW}_q}}(x_q,x'_q,z,z') &= G^{yy}_{A_{\mathrm{PPW}_o}}(x_q,x'_q,z,z') - G^{yy}_{A_{\mathrm{PPW}_o}}(x_q,x'_q,z,-z') \\
G^{xx}_{F_{\mathrm{PPW}_q}}(x_q,x'_q,z,z') &= G^{xx}_{F_{\mathrm{PPW}_o}}(x_q,x'_q,z,z') + G^{xx}_{F_{\mathrm{PPW}_o}}(x_q,x'_q,z,-z') \\
G^{zz}_{F_{\mathrm{PPW}_q}}(x_q,x'_q,z,z') &= G^{zz}_{F_{\mathrm{PPW}_o}}(x_q,x'_q,z,z') - G^{zz}_{F_{\mathrm{PPW}_o}}(x_q,x'_q,z,-z') \\
G_{W_{\mathrm{PPW}_q}}(x_q,x'_q,z,z') &= G_{W_{\mathrm{PPW}_o}}(x_q,x'_q,z,z') + G_{W_{\mathrm{PPW}_o}}(x_q,x'_q,z,-z')
\end{aligned} \tag{9}$$

The Green's functions for the internal equivalent problem inside the homogenous material objects are those corresponding to a free space two-dimensional problem filled with the constitutive parameters $(\epsilon_{d_q},\mu_{d_q})$.

Hence, these Green's functions are written in terms of second-kind zero-order Hankel functions as (Peterson et al., 1998b),

$$G_{\text{int}}(\vec{\rho}_q, \vec{\rho}'_q) = \frac{\xi_q}{4j} H_0^{(2)}\left(k_{d_q}|\vec{\rho}_q - \vec{\rho}'_q|\right) \tag{10}$$

being $k_{d_q} = \omega\sqrt{\varepsilon_{d_q}\mu_{d_q}}$, and $\xi = \mu_{d_q}$ for $G_{A_{\text{int}_q}}$, $\xi_q = \varepsilon_{d_q}$ for $G_{F_{\text{int}_q}}$, and $\xi = 1/\mu_{d_q}$ for $G_{W_{\text{int}_q}}$. Also, $|\vec{\rho}_q - \vec{\rho}'_q| = \sqrt{(x_q - x'_q)^2 + (z - z')^2}$ is the distance between source (x'_q, z') and observation points (x_q, z) in the inner equivalent problem (see Figure 4).

As can be seen in the relations between the electromagnetic fields and auxiliary potentials, given in equation (4), several differential operators are applied to the potential functions. These operators require the evaluation of spatial derivatives of the presented Green's functions. For the sake of space, the expressions of these Green's functions derivatives have not been included in this section, but they can be easily derived with the provided information.

2.2. Integral Equation Solution by the MoM

The system of integral equations outlined in section 2 is solved by the well-known MoM. In our particular implementation we have selected a Galerkin's approach with the same set of subsectional basis and testing functions (Harrington, 1968). An important simplification when dealing with inductive waveguide problems is that the unknown currents are distributed on the contours of the objects. Then, simple triangular subsectional basis and test functions, defined on the contours of the objects, give a robust implementation.

It is very important to note that, in order to achieve an efficient numerical implementation of the MoM solution, one has to compute the parallel plate Green's functions and their spatial derivatives in a fast way, since they are the key elements of the integral equation kernel. These Green's functions are represented, either in the spectral or in the spatial domains, as slowly convergent infinite series. In order to accelerate the evaluation of these series, different summation techniques proposed in the scientific literature can be applied, such as the Ewald Method (Capolino et al., 2005), the Kummer Transformation (Quesada Pereira et al., 2007), or other variations (Fructos et al., 2008). Nevertheless, this paper is not focused on the study of these acceleration procedures, but on the formulation of the integral equation for the analysis of rectangular waveguide discontinuities. In any case, we have chosen the Kummer Transformation as the acceleration technique for computing the parallel plate Green's functions, obtaining a good numerical performance. An efficient and optimal computational implementation of this integral equation yields to a very competitive alternative with respect to the use of commercial software tools such as HFSS, CST, or other numerical methods based on finite elements (Salazar Palma et al., 1998) or FDTD techniques (Peterson et al., 1998a). The main benefits of the proposed integral equation technique compared to other alternatives, are the limitation of the unknowns of the problem to the step discontinuity and to the contour of the arbitrarily shaped conducting and/or homogenous material objects inside the input/output rectangular waveguides. In fact, as shown in this paper, the rest of the problem and boundary conditions are taken into account by the formulated Green's functions.

2.3. Evaluation of the Scattering Parameters

Once the system of integral equations is solved by MoM, the last step is a postprocessing stage, employed to extract useful data from the numerical analysis of the structure under study. Interesting electrical parameters are the power response through the scattering parameters, or the evaluation of the electromagnetic fields in the whole structure. In this subsection we pay attention to the special procedure followed to compute the scattering parameters, being the computation of the electromagnetic fields useful to implement advanced design techniques, or for the study of power handling capabilities of the devices, which are out of the scope of this paper.

For the evaluation of the reflection coefficient (S_{11}), corresponding to the input waveguide fundamental mode $TE_{10}^{(1)}$, one has to compute the ratio between the reflected and incident electric field $\vec{E}^i$ at port 1. It is very important to note that in the equivalent problem 1, the total reflected electric field is computed as the addition of two different contributions, namely, the electric field scattered by the surface equivalent electric and magnetic currents $\vec{E}^s_{\text{PPW}_1}(\vec{J}_{C_1}, \vec{J}_{d_1}, \vec{M}_{d_1}, \vec{M}_{\text{ap}})$, and the image of the exciting electric field ($\vec{E}^i_{\text{imag}}$), traveling backward (see Figure 2). Moreover, since we are mainly interested in computing the power response with respect to the fundamental rectangular waveguide mode, one has to compute the line integral, along the port 1 cross

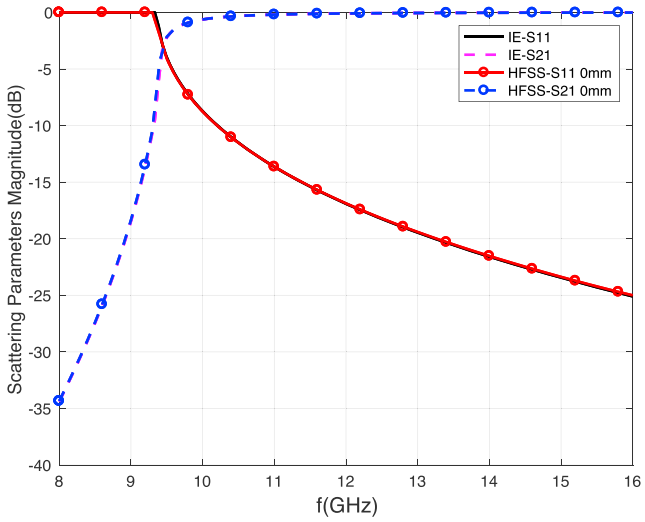

Figure 5. Step discontinuity with 0 mm offset. Dimensions in mm are $a_1 = 22.86$, $a_2 = 16$, constitutive parameters are $\epsilon_1 = \epsilon_2 = \epsilon_0$, $\mu_1 = \mu_2 = \mu_0$.

section (S_{p1}, see Figure 2), of the reflected electric field projected onto the normalized vector modal function $\vec{e}_{10}^{(1)}$ corresponding to the input rectangular waveguide mode $TE_{10}^{(1)}$, as shown next

$$S_{11} = \frac{\int_{S_{p1}} \left(\vec{E}^s_{\text{PPW}_1}(\vec{J}_{C_1}, \vec{J}_{d_1}, \vec{M}_{d_1}, \vec{M}_{\text{ap}}) + \vec{E}^i_{\text{imag}} \right) \cdot \vec{e}_{10}^{(1)} \text{d}x}{\int_{S_{p1}} \vec{E}^i \cdot \vec{e}_{10}^{(1)} \text{d}x} \quad . \tag{11}$$

In this expression, it is important to note the presence of the excitation image term ($\vec{E}^i_{\text{imag}}$) as part of the reflected field. We have verified that the results are incorrect if this image term is omitted from this expression.

On the other hand, the computation of the transmission coefficient (S_{21}) with respect to the output waveguide fundamental mode, is evaluated as the ratio between the scattered electric field at port2 $\vec{E}^s_{\text{PPW}_2}(\vec{J}_{C_2}, \vec{J}_{d_2}, \vec{M}_{d_2}, \vec{M}_{\text{ap}})$, and the excitation incident electric field $\vec{E}^i$ at port 1.

Since the computation of the scattering parameter S_{21} is carried out with respect to the fundamental mode (TE_{10}) of the input and output waveguides, one has to evaluate the line integral of the previous electric fields projected onto the normalized vector modal functions $\vec{e}_{10}^{(2)}$ and $\vec{e}_{10}^{(1)}$, along port 2 (S_{p2}, see Figure 3) and port 1 (S_{p1}, see Figure 2) cross sections, respectively. The final mathematical expression for the calculation of the S_{21} parameter is

$$S_{21} = \frac{\int_{S_{p2}} \vec{E}^s_{\text{PPW}_2}(\vec{J}_{C_2}, \vec{J}_{d_2}, \vec{M}_{d_2}, \vec{M}_{\text{ap}}) \cdot \vec{e}_{10}^{(2)} \text{d}x}{\int_{S_{p1}} \vec{E}^i \cdot \vec{e}_{10}^{(1)} \text{d}x} \quad . \tag{12}$$

Equations (11) and (12) can be easily modified if one needs to compute the multimodal response of the structure including other higher-order modes. The only changes will be that corresponding to the projections onto the normalized vector modal functions, now representing a given higher-order mode in the input $\vec{e}_{mn}^{(1)}$ and output $\vec{e}_{mn}^{(2)}$ waveguides, and the excitation of the problem. In this case, this excitation is not the fundamental mode and corresponds to a higher-order one and its image with respect to the perfect conductor condition at $z = 0$.

3. Results and Validation

In this section, different simulation examples are presented in order to validate the proposed integral equation formulation, and to show its usefulness and efficiency when compared to commercial software tools or other alternative numerical techniques. All the simulations have been performed in a computer with an Intel(R) Core(TM) i7-6700 CPU with clock frequency 3.4 GHz and RAM 32 GB.

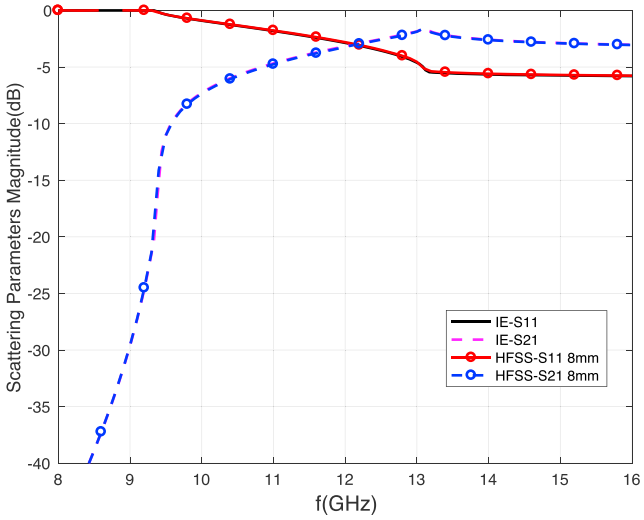

Figure 6. Step discontinuity with 8 mm offset. Dimensions in mm are $a_1 = 22.86$, $a_2 = 16$, constitutive parameters are $\epsilon_1 = \epsilon_2 = \epsilon_0$, $\mu_1 = \mu_2 = \mu_0$.

The first example is the analysis of a simple step discontinuity between two different empty waveguides filled with vacuum $\epsilon_1 = \epsilon_2 = \epsilon_0$ and $\mu_1 = \mu_2 = \mu_0$. The input waveguide is a standard WR-90 ($a_1 = 22.86$ mm $\times$ $b = 10.16$ mm), while the output waveguide has been chosen to have $a_2 = 16$ mm wide, with height $b = 10.16$ mm. The evaluation of the scattering parameters of the structure has been carried out for two different offsets, 0 mm and 8 mm (definition of the offset according to Figure 1).

The integral equation has been solved with only 15 basis functions for the expansion of the equivalent magnetic current surface density on the discontinuity, in both cases. Less than 30 terms are enough to achieve convergence for the evaluation of the parallel plate Green's functions series and their derivatives under the worst case scenario. For this structure, the simulation time was less than 0.05 s per frequency point. The simulation results have been compared to those provided by the HFSS finite elements full-wave commercial software, showing a very good agreement for the two different offsets (see Figures 5 and 6). The analysis has been carried out within a frequency range from 8 GHz to 16 GHz. Three different frequency regions can be differentiated in the results graph. In the first one, from 8 GHz to 9.375 GHz, the output waveguide is under cutoff, showing high return losses. The second region, from 9.375 GHz to 13.12 GHz, corresponds to the monomode propagation range in both waveguides. Finally, within the highest frequency range, from 13.12 GHz to 16 GHz, two modes are propagating in the input waveguide. Hence, a fraction of the fundamental mode excitation power is exchanged at the discontinuity, and is coupled to the second propagating mode in the input waveguide. As can be seen, this behavior is perfectly predicted by the expressions used to compute

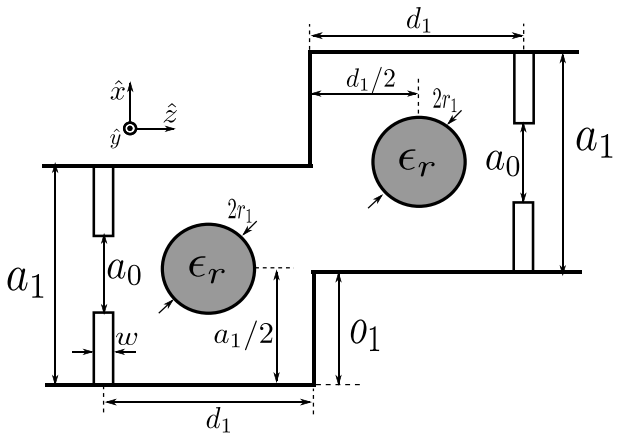

Figure 7. Second-order compact filter.

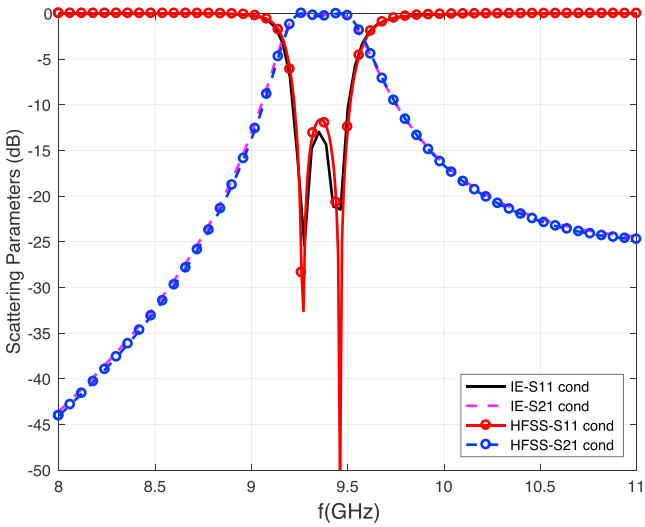

Figure 8. Response of a second-order band-pass filter with a fully metallic configuration. The dimensions in mm of the fully metallic filter are $a_1 = 22.86$, $a_0 = 11.46$, $w = 2$, $d_1 = 20$, and $O_1 = 12.6$.

the scattering parameters [see equations (11) and(12)]. These expressions allow for the evaluation of the scattering parameters with respect to a given propagating mode used as reference, which in our case is taken as the fundamental one.

The next design is a second-order band-pass filter, that consists of two cavities coupled by an iris, and configured with a given offset between the input and output waveguide sections (see Figure 7). Two different realizations of the filter have been considered. First, the band-pass filter has been designed with only empty cavities filled with vacuum. These cavities are formed by an input/output conducting inductive window iris, and the aperture corresponding to the step discontinuity. Only 65 basis functions have been used for modeling the irises (28 each one) and the discontinuity (9). The Green's functions have been computed with less than 30 terms. For this fully metallic configuration, the computation time per frequency point was less than 0.08 s. The second design is similar to the previous one, but placing two dielectric circular posts at the center of each cavity. As expected, the effect of the dielectric posts reduces the effective size of the cavities, if the filter response is kept with the same passband and bandwidth as the original one, which is used as reference. This is a classical procedure for designing compact size filters, at the expense of increasing the final insertion

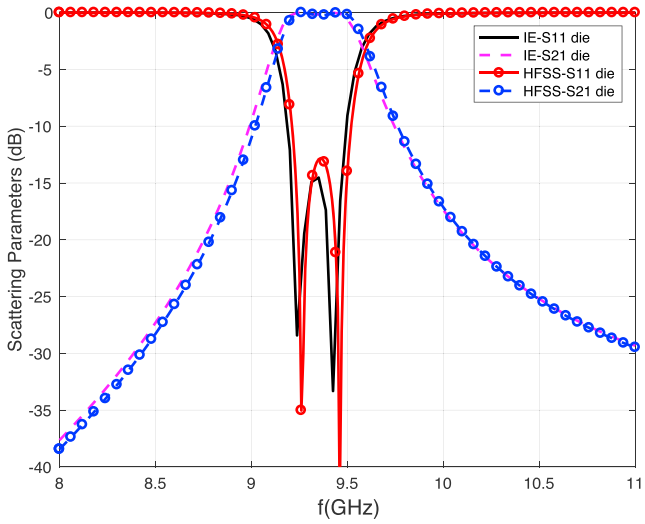

Figure 9. Response of a second-order band-pass filter having dielectric circular posts at the center of the cavities. The dimensions in mm of the compact size filter with lossless dielectric posts ($\epsilon_r = 3.95$) are $a_1 = 22.86$, $a_0 = 11.46$, $w = 2$, $d_1 = 10.6$, $r_1 = 3$, and $O_1 = 12.7$.

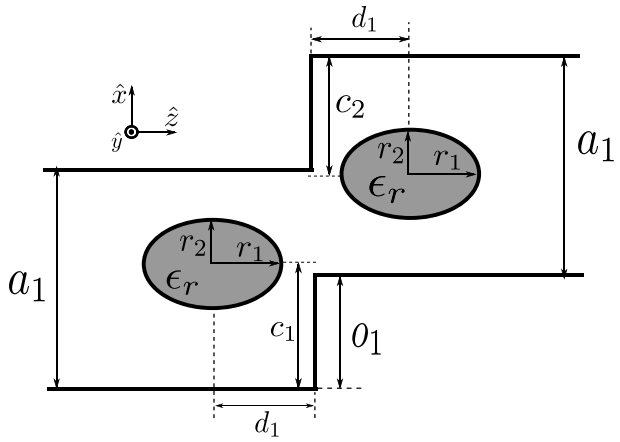

Figure 10. Geometry of a fourth-order filter with two transmission zeros composed of two coupled dielectric resonators and a step discontinuity.

losses due to the additional losses introduced by the dielectric materials. For this second design, 120 additional basis functions have been employed for the expansion of the electric and magnetic equivalent currents on the dielectric post contours, being the total number of unknowns is 185. In this second case, the simulation time, 0.65 s per frequency point, is higher due to the increased number of unknowns and additional Green's functions components that have to be computed.

The response of the second-order filter has been computed with the novel integral equation formulation in the frequency range from 8 GHz to 11 GHz (see Figures 8 and 9), for both configurations (fully metallic and with dielectric posts). The obtained simulation results have been compared to those computed by the commercial software HFSS, showing a very good agreement for both designs. This last validation confirms that the proposed integral equation can be used in order to analyze complex structures, including combinations of arbitrarily shaped metallic posts and homogenous material bodies.

The last example is a band-pass filter composed of only dielectric elliptical posts and a step discontinuity (see Figure 10). In this case, the dimensions and the dielectric permittivity are adjusted in order to obtain a higher fractional bandwidth (up to 10%–12%) with respect to the previously presented design. This characteristic is due to the presence of four pole resonances and two transmission zeros that could be properly combined to achieve a broad band-pass response with high selectivity. Since the goal of this paper is only to show

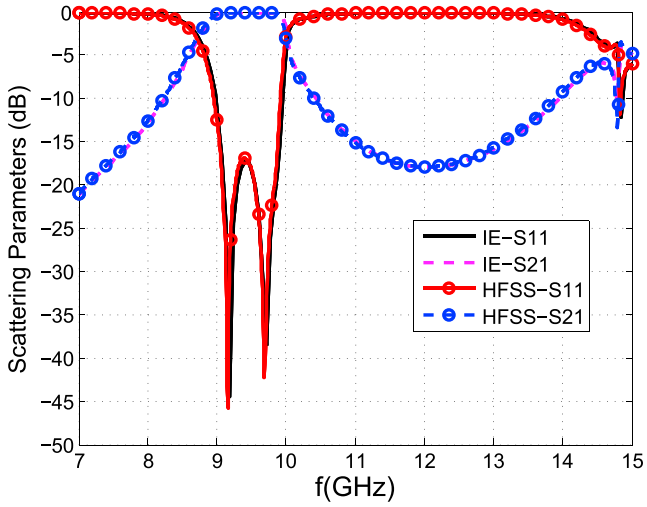

Figure 11. Response of a fourth-order filter composed of only dielectric posts ($\epsilon_r = 9$) and a step discontinuity with only complex transmission zeros and two real poles. The dimensions of this design in mm are $a_1 = 22.86$, $d_1 = 5$, $c_1 = c_2 = a_1/2 = 11.43$, $r_1 = 4$, $r_2 = 3.75$, and $O_1 = 7.5$.

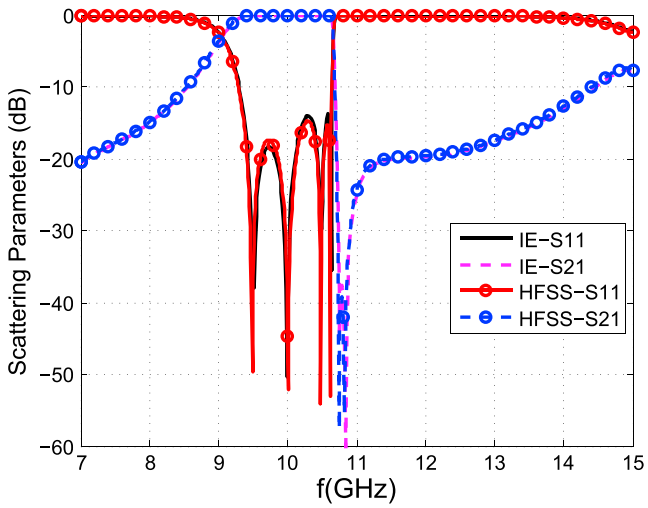

Figure 12. Response of fourth-order filter composed of only dielectric posts ($\epsilon_r = 9$) and a step discontinuity (four poles and two transmission zeros in the real frequency axis). The dimensions of this design in mm are $a_1 = 22.86$, $d_1 = 4.05$, $c_1 = 11.53$, $c_2 = 11.33$, $r_1 = 4$, $r_2 = 3.5$, and $O_1 = 8.39$.

the versatility and efficiency of the proposed integral equation formulation, and therefore it is not focused on filter design and optimization techniques, just two preliminary configurations are considered and analyzed.

The first filter implementation gives a response where only two poles are in the real frequency axis, while the transmission zeros are complex, as can be seen in the results of Figure 11.

The second filter design results in a response where the four poles are in the real frequency axis, and two transmission zeros are also real, thus improving the selectivity close to the upper cutoff frequency (see Figure 12). To obtain these responses, a high dielectric relative permittivity value ($\epsilon_r = 9$) has been assigned to the elliptical posts. The main benefit of this last kind of filter realization is a compact size, and the possibility to realize high order and selective responses with reduced number of filter elements. As a drawback, the optimization and design procedures are difficult, due to the strong couplings of the different elements of the filter structure. In any case, it is important to observe the very good agreement obtained in Figures 11and 12 with respect to the commercial software HFSS, thus further validating the integral equation formulation presented in this paper. In this simulation, only 129 basis functions have been employed for expansion of the unknowns corresponding to the dielectric posts (60 each one) and the step aperture (9). Once more, only 30 terms are needed at most for computing the accelerated Green's functions. The computation time has been 0.38 s for frequency point, which is very convenient for further design procedures.

Although, the presented examples are limited to rectangular, circular, and elliptical geometries for the obstacles, any other kind of shape could be considered due to the particular numerical solution of the proposed integral equation by the MoM. Consequently, any complex geometry that can be discretized with linear segments can be treated with the proposed numerical implementation.

4. Conclusions and Future Work

In this paper, a novel spatial domain integral formulation that allows a full-wave characterization of step discontinuities between different rectangular waveguides has been presented. The proposed formulation takes easily into account the presence of a given number of arbitrarily shaped conducting and/or homogenous material posts in the vicinity of the step. The kernel of the final system of integral equations is written in terms of the input/output parallel plate Green's functions, in addition to a spatial image with respect to a ground plane located at the discontinuity. The solution of the resulting integral equation is efficiently carried out by means of the MoM, after the application of specific acceleration techniques for computing the infinite series used to formulate the Green's functions of the problem. The numerical technique is very competitive in relation to current commercial software packages or other alternative methods such as finite elements or FDTD, since the unknowns of the equivalent problem are reduced to the discontinuity aperture and the arbitrarily shaped post contours. Different practical simulation examples have been presented in order to show

the validity, efficiency, and usefulness of the novel integral equation. A simple step discontinuity between two rectangular waveguides considering two different offsets, and a second-order filter composed of two rectangular cavities coupled by a step have been discussed. This latter example has been analyzed with two different configurations, one of them considering empty cavities and the other one taking into account the presence of dielectric circular posts that reduce the global size of the filter. The last studied structure was a step discontinuity with two coupled elliptic dielectric resonators placed on each side. It has been shown that a fourth-order response, including also two transmission zeros, could be obtained after an optimization procedure. In all cases, the agreement between the proposed technique and commercial software tools has been very good, and with good computational performances. In this manner, we have shown the usefulness, accuracy, and versatility of the integral equation formulation proposed in this paper.

Although, the integral equation formulation can be particularized for two-dimensional or capacitive rectangular waveguide discontinuities, this work has been focused on the simpler study of inductive steps, leaving its extension to the other possible configurations as a future research work.

Acknowledgments
This research work has been financially supported by the Spanish *Ministerio de Economía y Competitividad* in the frame of the projects "Demostradores Tecnológicos de Filtros y Multiplexores con Respuestas Selectivas y Sintonizables en Nuevas Guías Compactas para Aplicaciones Espaciales (COMPASSES)" with Ref. TEC2016-75934-C4-1-R, and "Análisis y Diseño de Nuevos Componentes en Microondas y Milimétricas para Comunicaciones por Satélite (MILISAT)" with Ref. TEC2016-75934-C4-4-R. As an additional financial source we thank the regional agency Fundación Séneca from Región de Murcia under the research project "Desarrollo de Antenas y Componentes Pasivos de Microondas para Sistemas Avanzados de Comunicaciones" with Ref. 19494/PI/14 and Ref. 20147/EE/17, and the PhD scholarship granted by the Spanish national *Ministerio de Educación, Cultura y Deporte* with Ref. FPU15/02883. All results of this paper can be reproduced by using the data and information contained in the drawings and in the captions of the figures included in the paper.

References

Arcioni, P., Bressan, M., Conciauro, G., & Perregrini, L. (1997). Generalized Y-matrix of arbitrary H-plane waveguide junctions by the BI-RME method. In *IEEE MTT-S International Microwave Symposium Digest* (pp. 211–214). Denver.

Balanis, C. A. (1989). *Advanced engineering electromagnetics*. Hoboken, NJ: John Wiley.

Cameron, R. J., Kudsia, C. M., & Mansour, R. R. (2007). *Microwave filters for communication systems* (pp. 431–467). Hoboken, NJ: John Wiley.

Capolino, F., Wilton, D. R., & Johnson, W. A. (2005). Efficient computation of the 2-D Green's function for 1-D periodic structures using the Ewald method. *IEEE Transactions on Antennas and Propagation*, *53*(9), 2977–2984.

Catina, V., Arndt, F., & Brandt, J. (2005). Hybrid surface integral-equation/mode-matching method for the analysis of dielectric loaded waveguide filters of arbitrary shape. *IEEE Transactions on Microwave Theory and Techniques*, *53*(11), 3562–3567.

Fructos, A. L., Boix, R. R., Mesa, F., & Medina, F. (2008). An efficient approach for the computation of 2-D Green's functions with 1-D and 2-D periodicities in homogeneous media. *IEEE Transactions on Antennas and Propagation*, *56*(12), 3733–3742. https://doi.org/10.1109/TAP.2008.2007281

Guglielmi, M., & Newport, C. (1990). Rigorous, multimode equivalent network representation of inductive discontinuities. *IEEE Transactions on Microwave Theory and Techniques*, *38*(11), 1651–1659. https://doi.org/10.1109/22.60012

Harrington, R. F. (1968). *Field computation by moment methods*. Hoboken, NJ: John Wiley.

Hu, Y. L., Li, J., Ding, D. Z., & Chen, R. S. (2016). Analysis of transient EM scattering from penetrable objects by time domain nonconformal VIE. *IEEE Transactions on Antennas and Propagation*, *64*(1), 360–365. https://doi.org/10.1109/TAP.2015.2501437

Marcuvitz, N. (1964). *Waveguide handbook*, MIT Radiation Laboratory Series. Boston, Massachusetts, USA: Boston Technical Publisher.

Mohsen, K., & Kian, P. (2017). Analysing metamaterial layer by simpler approach based on mode matching technique. *IET Microwaves Antennas and Propagation*, *11*(5), 607–616.

Mrvic, M., Potrebic, M., & Tosic, D. (2016). Compact E plane waveguide filter with multiple stopbands. *Radio Science*, *51*, 1895–1904. https://doi.org/10.1002/2016RS006169

Perez Soler, F., Quesada Pereira, F., Canete Rebenaque, D., Pascual Garcia, J., & Alvarez Melcon, A. (2007). Efficient integral equation formulation for inductive waveguide components with posts touching the waveguide walls. *Radio Science*, *42*, RS6002. https://doi.org/10.1029/2006RS003591

Peterson, A. F., Ray, S. L., & Mittra, R. (1998a). *Finite-difference time-domain methods on orthogonal meshes* (pp. 495–523). Hoboken, NJ: John Wiley. https://doi.org/10.1109/9780470544303.ch12

Peterson, A. F., Ray, S. L., & Mittra, R. (1998b). *Computational methods for electromagnetics* (p. 7). Hoboken, NJ: John Wiley.

Poggio, A. J., & Miller, E. K. (1973). *Integral equation solutions of three-dimensional scattering problems*. Oxford: Pergamon Press.

Quesada Pereira, F., Boria, V. E., Gimeno, B., Cañete Rebenaque, D., Pascual Garcia, J., & Alvarez Melcon, A. (2006). Investigation of multipaction phenomena in inductively coupled passive waveguide components for space applications. In *IEEE MTT-S International Microwave Symposium Digest* (pp. 246–249). San Francisco, CA.

Quesada Pereira, F., Boria Esbert, V. E., Pascual Garcia, J., Vidal Pantaleoni, A., Alvarez Melcon, A., Gomez Tornero, J., & Gimeno, B. (2007). Efficient analysis of arbitrarily shaped inductive obstacles in rectangular waveguides using a surface integral equation formulation. *IEEE Transactions on Microwave Theory and Techniques*, *55*(4), 715–721.

Quesada Pereira, F. D., Vera Castejón, P., Alvarez Melcon, A., Gimeno Martínez, B., & Boria Esbert, V. E. (2011). An efficient integral equation technique for the analysis of arbitrarily shaped capacitive waveguide circuits. *Radio Science*, *46*, RS2017. https://doi.org/10.1029/2010RS004458

Salazar Palma, M., Sarkar, T. K., Garcia Castillo, L. E., Roy, T., & Djordjevic, A. (1998). *Iterative and self-adaptive finite elements in electromagnetic modeling*. Norwood, MA: Artech House, Inc.

Stumpf, M., & Leone, M. (2009). Efficient 2-D integral equation approach for the analysis of power bus structures with arbitrary shape. *IEEE Transactions on Electromagnetic Compatibility*, *51*(1), 38–45. https://doi.org/10.1109/TEMC. 2008.2009223

Wei, X. C., Li, E. P., Liu, E. X., & Cui, X. (2008). Efficient modeling of rerouted return currents in multilayered power-ground planes by using integral equation. *IEEE Transactions on Electromagnetic Compatibility*, *50*(3), 740–743. https://doi.org/10.1109/TEMC.2008.924392

Zhao, H., Liu, E. X., Hu, J., & Li, E. P. (2014). Fast contour integral equation method for wideband power integrity analysis. *IEEE Transactions on Components, Packaging and Manufacturing Technology*, *4*(8), 1317–1324. https://doi.org/10.1109/TCPMT.2014.2327242